ORIGINAL ARTICLE

Interleukin-17A and interleukin-22 production by conventional and non-conventional lymphocytes in three different end-stage lung diseases

Melanie Albrecht[1,2,3†], Olga Halle[1,3†] (iD), Svenja Gaedcke[3], Sophia T Pallenberg[1], Julia Camargo Neumann[1], Marius Witt[1], Johanna Roediger[1], Marina Schumacher[1], Adan Chari Jirmo[1,3], Gregor Warnecke[3,4], Danny Jonigk[3,5], Peter Braubach[3,5], David DeLuca[3], Gesine Hansen[1,3] & Anna-Maria Dittrich[1,3] (iD)

[1]Pediatric Pneumology, Allergology and Neonatology, Hannover Medical School, Hannover, Germany
[2]Molecular Allergology, Paul-Ehrlich-Institut, Federal Institute for Vaccines and Biomedicines, Langen, Germany
[3]Biomedical Research in Endstage and Obstructive Lung Diseases (BREATH), German Center for Lung Research (DZL), Hannover, Germany
[4]Department of Cardiac Surgery, Heidelberg Medical School, Heidelberg, Germany
[5]Institute of Pathology, Hannover Medical School, Hannover, Germany

Correspondence

A-M Dittrich, Pediatric Pneumology,
Allergology and Neonatology,
Hannover Medical School,
Hannover 30625, Germany.
E-mail: dittrich.anna-maria@mh-hannover.de

[†]Equal contributors.

Abstract

Objectives. The contribution of adaptive *vs.* innate lymphocytes to IL-17A and IL-22 secretion at the end stage of chronic lung diseases remains largely unexplored. In order to uncover tissue- and disease-specific secretion patterns, we compared production patterns of IL-17A and IL-22 in three different human end-stage lung disease entities. **Methods.** Production of IL-17A, IL-22 and associated cytokines was assessed in supernatants of re-stimulated lymphocytes by multiplex assays and multicolour flow cytometry of conventional T cells, iNKT cells, $\gamma\delta$ T cells and innate lymphoid cells in bronchial lymph node and lung tissue from patients with emphysema ($n = 19$), idiopathic pulmonary fibrosis ($n = 14$) and cystic fibrosis ($n = 23$), as well as lung donors ($n = 17$). **Results.** We detected secretion of IL-17A and IL-22 by CD4$^+$ T cells, CD8$^+$ T cells, innate lymphoid cells, $\gamma\delta$ T cells and iNKT cells in all end-stage lung disease entities. Our analyses revealed disease-specific contributions of individual lymphocyte subpopulations to cytokine secretion patterns. We furthermore found the high levels of microbial detection in CF samples to associate with a more pronounced IL-17A signature upon antigen-specific and unspecific re-stimulation compared to other disease entities and lung donors. **Conclusion.** Our results show that both adaptive and innate lymphocyte populations contribute to IL-17A-dependent pathologies in different end-stage lung disease entities, where they establish an IL-17A-rich microenvironment. Microbial colonisation patterns and cytokine secretion upon microbial re-stimulation suggest that pathogens drive IL-17A secretion patterns in end-stage lung disease.

INTRODUCTION

Interleukin (IL)-17A and interleukin-22 both exert critical functions in airway defence, lung repair and lung homeostasis. IL-17A plays a crucial role in the protection against pulmonary pathogens, particularly *Pseudomonas aeruginosa* (*P.a.*), *Staphylococcus aureus* (*S.a.*)[1] and fungi,[2] while IL-22 modulates epithelial function promoting host defence and repair mechanisms in the airways.[1,3] Both IL-17A and IL-22 can contribute to the development of bronchus-associated tissue (BALT).[4–6] In lymph nodes and BALT, IL-17A has been implicated in germinal centre (GC) B-cell development and monocyte–macrophage differentiation, leading to antibody formation and TGF-β secretion, capable of driving fibrosis.[7–9] IL-22 has been implicated in the recruitment of B cells to BALT.[6] In murine models, IL-17A can initiate and propagate acute lung injury[10,11] and the development of fibrosis,[9,12–14] mechanisms which most likely underlie its association with unfavorable outcomes in different pulmonary disease entities.[1] IL-17A might thus contribute to the fibrotic changes that characterise various pulmonary diseases in their end stage, constituting a converging pathway of end-stage lung disease.

Secretion of IL-17A was originally identified in conventional CD3+CD4+ T helper (Th) lymphocytes,[15] but has been detected – oftentimes alongside and co-secreted with IL-22 – in other conventional and non-conventional T cells, such as CD3+CD8+ T cells, innate lymphoid cells, γδ T cells and invariant natural killer T (iNKT) cells,[16] all of which show a propensity to reside in non-lymphoid tissue and in the submucosa.[17] IL-17A secretion by non-Th17 cells has been causally linked to the failure to clear pneumotropic pathogens and to the development of fibrosis in different mouse models.[18–20] These studies suggest that the cellular source of IL-17A can critically determine outcomes in some disease processes.[21] We have recently identified IL-17A secretion by Th cells, CD8+ T cells and several innate lymphocyte populations, that is γδ T cells, iNKT and innate lymphoid cells, in cystic fibrosis (CF) patients. Moreover, we were able to assign a critical role for IL-17A secretion in the development of airway inflammation and pulmonary tissue destruction in CF-like murine lung disease,[22] suggesting mechanisms by which IL-17A might critically contribute to progression towards end-stage disease in CF.

However, in the context of other diseases leading to end-stage lung diseases, such as emphysema and fibrosis, secretion of IL-17A or IL-22 by lymphocytes other than Th17 cells remains poorly delineated. With the study presented here, we aimed to identify the contribution of conventional and non-CD3+CD4+ lymphocytes to IL-17A and IL-22 secretion in lung tissue and draining bronchial lymph nodes in three end-stage lung disease entities commonly requiring lung transplantation: CF, emphysema and idiopathic fibrosis. We analysed pathogen-specific secretion of IL-17A and IL-22 in these end-stage lung diseases and associated their secretion pattern with the detection of typical pathogens found in chronic lung diseases to address the role of these pathogens in driving IL-17A and IL-22 secretion.

RESULTS

Patient characteristics

We obtained samples from total 56 patients suffering from CF ($n = 23$), lung emphysema ($n = 19$) or pulmonary fibrosis ($n = 14$), respectively (Table 1, Supplementary figure 1). These samples included 40 bronchial lymph node (LN) samples, from CF ($n = 18$), emphysema ($n = 10$) and fibrosis patients ($n = 12$), and a total of 34 lung tissue (LT) samples from CF ($n = 11$), emphysema ($n = 15$) and fibrosis patients ($n = 8$) (Table 1). Tracheal lymph nodes resected during the transplantation process were obtained from $n = 17$ lung donors (LD), as a comparator for the *in vivo* situation in people not affected by pulmonary disease. CF patients were significantly younger (27 ± 10 years) than fibrosis (54 ± 9 years) and emphysema (57 ± 4 years) patients (Supplementary figure 1a) with no significant difference in gender distribution among the three disease entities (Supplementary figure 1b). Because of ethical constraints, neither age nor gender could be obtained from LD. Culture-dependent analyses of bronchial secretions

obtained intra-operatively during transplantation revealed higher percentages of samples with the detection of *S.a.*, fungi and other specific bacterial species in CF samples than emphysema and fibrosis samples (Supplementary figure 1c, Table 1). *P.a.* was detected exclusively in CF samples (Supplementary figure 1c, Table 1).

IL-17A and IL-22 are produced in lymph nodes and lung tissue of different end-stage lung diseases

The production of IL-17A and IL-22 was detectable in the supernatants of PMA/ionomycin-stimulated single-cell suspensions from LT and LN in all three different end-stage lung diseases and in LN from LD (Figure 1a and b). Comparing disease entities, both IL-17A production and IL-22 production were highest in fibrosis LT and in CF LN, and lowest in emphysema LT and fibrosis LN, corroborating previous studies, which identified an 'IL-17 signature' in CF lung disease.[23–26] Average IL-17A and IL-22 concentrations in LN from LD were comparable to those in emphysema LN and by trend higher than IL-17 and IL-22 concentrations in fibrosis LN. In LT from CF and fibrosis, as well as in LN from CF and LD, we determined a high and significant correlation between IL-17A and IL-22 secretion (Figure 1c and d), suggesting an environment influenced by secretion of both of these cytokines. By contrast, correlation of IL-17A and IL-22 levels was weaker in fibrosis LN and emphysema LT and LN. Together, these observations indicate that a microenvironment influenced by both IL-17A and IL-22 characterises LT and LN from different end-stage lung diseases, with a particular propensity for IL-17A and IL-22 (co-)secretion in tissues from CF patients.

The IL-17A microenvironment in end-stage lung disease is shaped by non-conventional lymphocytes in a disease-specific manner

To confirm the presence of IL-17A-secreting lymphocytes in LT and LN *in situ*, we performed immunofluorescence staining of cryosections prepared from these tissues. IL-17A-producing cells were detected in all tissues, regardless of disease entity (Figure 2a and b). In LT, IL-17A$^+$ cells were typically located in lymphocyte-rich aggregates that were often associated with or found in the vicinity of the airways. In LNs, IL-17A$^+$ cells were typically, but not exclusively,

found in the T-cell zone. Interestingly, IL-17A expression was not exclusive to CD3$^+$ lymphocytes (white arrowheads) in any of the tissues, but we also found IL-17 expression on a substantial number of CD3-negative mononuclear cells (yellow arrowheads, Figure 2a and b), suggesting that both T cells and non-T lymphocytes contribute to IL-17A production in end-stage LT and LN.

Based on these findings, we consecutively employed flow cytometric analysis to pinpoint the contributions of individual lymphocyte subpopulations to the overall IL-17A or IL-22 secretion and IL-17A/IL-22 co-secretion (refer to Supplementary figure 2 for panels and complete gating strategy). Regardless of disease entity and tissue origin, for all of these cytokine-secreting subpopulations, conventional CD3$^+$CD4$^+$ T cells were the most frequent subpopulation. However, conventional CD3$^+$CD4$^+$ T cells constituted less than 50% of IL-17A-producing lymphocytes in LT and at most 70% in LN (Figure 2c and d). Regardless of disease entity, at least 10% and up to 60% of the lymphocytes in LT and at least 20% and up to 50% of the lymphocytes in LN contributing to the secretion of IL-17, IL-17A/IL-22 and IL-22 were non-CD3$^+$CD4$^+$ cells (Figure 2c and d), suggesting substantial contributions of non-CD3$^+$CD4$^+$ lymphocytes to IL-17A and/or IL-22 production in end-stage lung diseases.

The specific identity of IL-17- and IL-22-producing non-CD3$^+$CD4$^+$ lymphocytes varied with disease entity. Among IL-17A$^+$ cells in LT, CD3$^+$CD8$^+$ lymphocytes dominated in emphysema and fibrosis, but were considerably less frequent in CF samples (LT, IL-17A$^+$, red-filled sub-bars, Figure 2c). Among IL-17A/IL-22 double producers in LT, we detected iNKT cells and CD8$^+$ T cells, with iNKT cells being more frequent in CF than in the other two disease entities (LT, IL-17A$^+$IL-22$^+$, grey-filled sub-bars, Figure 2c). Among IL-22 producers in LT, γδ T cells were prevalent, particularly in samples from CF and emphysema patients (LT, IL-22$^+$, blue-filled sub-bars, Figure 2c), and, particularly in CF samples, innate lymphoid cells (ILCs) also contributed to IL-22 production in LT (Figure 2c and d, green-filled sub-bars).

In LN samples, iNKT cells and CD3$^+$CD8$^+$ T cells contributed to cytokine production next to the most frequent CD3$^+$CD4$^+$ T cells, particularly within the IL-22-producing population (Figure 2d, grey-filled and red-filled sub-bars). In LN samples from CF tissues, we additionally found a

Table 1. Detection of specific pathogens in airways of patients at time of lung transplant

	Sex	Age	Disease	*Pseudomonas aeruginosa*	*Staphylococcus aureus*	Fungi[a]	Other[b]	LT	LN
1	f	15	CF	+	neg	neg	+		×
2	f	46	CF	+	neg	neg	+		×
3	m	17	CF	neg	+	neg	+		×
4	f	24	CF	+	neg	neg	neg		×
5	f	28	CF	neg	neg	neg	+		×
6	m	35	CF	+	+	+	neg		×
7	m	15	CF	+	neg	neg	neg		×
8	m	27	CF	+	neg	+	+		×
9	m	30	CF	+	+	neg	+		×
10	f	34	CF	neg	neg	+	+	×	
11	m	15	CF	+	+	neg	neg	×	×
12	f	26	CF	+	+	neg	neg	×	×
13	m	30	CF	+	neg	neg	neg	×	×
14	m	36	CF	+	neg	+	+	×	
15	f	23	CF	+	neg	+	neg	×	×
16	f	31	CF	+	+	neg	+	×	
17	f	25	CF	neg	+	+	+		×
18	m	46	CF	+	neg	+	+		×
19	f	23	CF	+	neg	+	neg	×	×
20	f	7	CF	neg	neg	neg	+		×
21	m	44	CF	+	neg	+	+	×	
22	f	23	CF	+	neg	+	neg	×	
23	m	21	CF	+	+	+	neg	×	×
1	m	52	Emphy	neg	neg	neg	neg	×	×
2	m	60	Emphy	neg	neg	neg	+		×
3	f	54	Emphy	neg	neg	+	+		×
4	m	62	Emphy	neg	neg	neg	neg	×	×
5	f	59	Emphy	neg	neg	neg	neg	×	×
6	m	61	Emphy	neg	neg	neg	neg	×	
7	m	49	Emphy	neg	neg	+	neg	×	
8	m	59	Emphy	neg	neg	+	neg	×	
9	f	54	Emphy	neg	neg	+	+	×	
10	f	58	Emphy	neg	neg	neg	+	×	
11	f	60	Emphy	neg	neg	neg	neg	×	
12	f	60	Emphy	N.D.	N.D.	N.D.	N.D.		×
13	m	58	Emphy	neg	neg	neg	neg	×	×
14	m	61	Emphy	neg	neg	neg	neg	×	×
15	f	58	Emphy	neg	neg	neg	neg		×
16	f	54	Emphy	neg	neg	neg	neg	×	×
17	f	61	Emphy	N.D.	N.D.	N.D.	N.D.	×	
18	m	49	Emphy	N.D.	N.D.	N.D.	N.D.	×	
19	m	55	Emphy	N.D.	N.D.	N.D.	N.D.	×	
1	m	50	Fibro	neg	neg	neg	+		×
2	f	62	Fibro	neg	neg	neg	neg		×
3	m	59	Fibro	neg	neg	+	+	×	
4	m	45	Fibro	neg	+	+	neg	×	×
5	m	53	Fibro	neg	+	neg	+	×	
6	m	56	Fibro	neg	+	neg	neg		×
7	f	45	Fibro	neg	neg	+	neg		×
8	m	62	Fibro	neg	neg	+	neg	×	×
9	m	64	Fibro	neg	neg	+	neg		×
10	m	57	Fibro	neg	neg	+	neg	×	×
11	m	61	Fibro	neg	neg	neg	+		×
12	m	46	Fibro	neg	neg	neg	neg	×	×
13	m	58	Fibro	neg	neg	neg	neg	×	×

(Continued)

Table 1. Continued.

	Sex	Age	Disease	Pseudomonas aeruginosa	Staphylococcus aureus	Fungi[a]	Other[b]	LT	LN
14	f	32	Fibro	neg	neg	neg	neg	×	×
1	Unknown	Unknown	LD	N.D.					×
2			LD						×
3			LD						×
4			LD						×
5			LD						×
6			LD						×
7			LD						×
8			LD						×
9			LD						×
10			LD						×
11			LD						×
12			LD						×
13			LD						×
14			LD						×
15			LD						×
16			LD						×
17			LD						×

+, positive culture; CF, cystic fibrosis; Emphy, lung emphysema; f, female; Fibro, pulmonary fibrosis; LD, lung donor; LN, lymph node; LT, lung tissue; m, male; N.D., no culture performed; neg, negative culture.

Pathogens were detected according to routine standard microbiological practice for the detection of bacteria and fungi in bronchial secretions obtained by intra-operative collection at the time of lung transplant. Columns 'LT' and 'LN' indicate from which patients' lung tissue (LT) and lymph node tissue (LN) were included in the analysis, with × designating samples included from the respective source. LD sex and age are unknown for ethical reasons. Four emphysema samples have unknown sex and age and were not subjected to microbiological analysis but to cluster analysis only.

[a]Aspergillus, Saccharomyces, Candida and Wangiella species.

[b]Achromobacter, Burkholderia, Stenotrophomonas, Enterococcus, Serratia, Escherichia, Enterobacter, Haemophilus and Klebsiella species.

substantial proportion of ILCs within the IL-22+ population (green-filled sub-bars, Figure 2d), whereas in LN samples from fibrosis tissues, next to CD4+ T cells, iNKT cells were most frequent among IL-17A and IL-17A+IL-22+ secretors (grey-filled sub-bars, Figure 2d). Altogether, these data suggest that non-Th17 cells contribute substantially to IL-17A and IL-22 secretion in the inflammatory environment in end-stage lungs and that the contribution of specific non-Th17 subpopulations to overall IL-17A or IL-22 secretion differs between the disease entities: CF, fibrosis and emphysema.

Clustering identifies disease-specific subpopulations and suggests conserved and redundant IL-17A production across end-stage lung disease entities

To identify specific cellular phenotypes among the lymphocyte subpopulations capable of secreting IL-17A and/or IL-22, that is among CD4+ T cells, CD8+ T cell, gd T cells, iNKT cells or ILCs, we analysed these subpopulations by Uniform Manifold Approximation and Projection (UMAP) and Gaussian Mixture Models (GMM). In detail, we subdivided lymphocytes in the flow cytometric data sets into CD4+ T cells, CD8+ T cells, $\gamma\delta$ T cells, iNKT cells and ILCs by manual gating and consecutively performed clustering on identical cell numbers from all disease entities (Figure 3a and b, 'all entities'), incorporating all markers included in the flow cytometry panel (for a complete list of markers and for gating strategy, refer to the Methods section and Supplementary figure 2). Consecutively, clusters were stratified according to disease entity and cells originating from the individual diseases were depicted in separate panels (Figure 3a and b, panels 'CF', 'Emphy' and 'Fibro', respectively). These analyses permit the identification and relative quantification of cells characterised by a similar profile of expression marker combinations within a given subpopulation, that is among ILCs, $\gamma\delta$ T cells, iNKT, CD3+CD8+ or CD3+CD4+ cells, including the relative IL-17A or IL-22 expression of a given subcluster in comparison with other subclusters. They thus permit to identify disease-specific
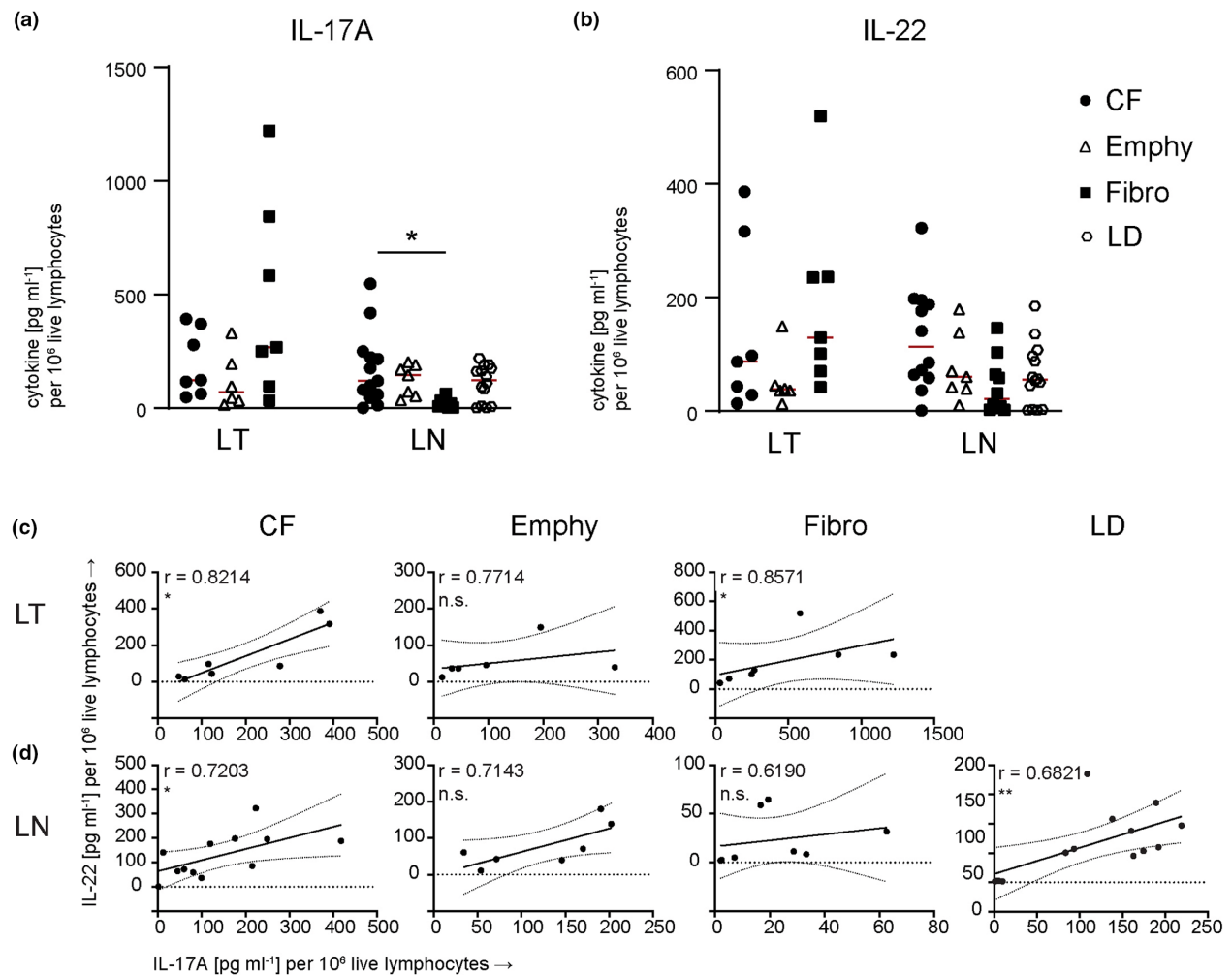
Figure 1. IL-17A and IL-22 are produced in lymph nodes and lung tissue of different end-stage lung diseases **(a)** IL-17A and **(b)** IL-22 concentrations in PMA/ionomycin-re-stimulated supernatants of cells obtained from lung (LT) and lymph node tissue (LN) of patients with the indicated end-stage lung diseases cystic fibrosis (CF), emphysema (Emphy), idiopathic pulmonary fibrosis (Fibro), or from lung donors (LD). Every dot indicates one patient, horizontal lines indicate the mean. Concentration values were normalised across samples to the proportion of lymphocytes among live cells as determined by flow cytometry. A Kruskal–Wallis test was performed with Dunn's multiple comparison analysis. **(c)** Spearman non-parametric correlation of IL-17A and IL-22 secretion in LT and **(d)** LN samples shown in **a** and **b**. Dotted lines show 95% confidence band. *r* = Spearman correlation coefficient, asterisks denote *P*-values for correlation.

differences concerning the subpopulation-specific clusters.

Our clustering analyses revealed that certain clusters within a specific lymphocyte subpopulation occurred predominantly or even exclusively in certain diseases (Figure 3a and b). In particular, a specific subpopulation of γδ T cells was present in LT of CF and fibrosis, but not emphysema patients (γδ T cell cluster 3, Figure 3a), and iNKT cell cluster 3 was present in fibrosis only, but not in CF and emphysema (iNKT cell cluster 3, Figure 3a). Because of small cell numbers in LT, analyses of ILCs precluded

comparisons in a disease-specific manner (Figure 3a, ILC panels). Also in LT, CD3⁺CD8⁺ T-cell clusters 0, 3 and 4 were found mainly in CF and fibrosis samples, rather than in emphysema (Figure 3a, CD3⁺CD8⁺ panels). Among LT CD4⁺ T cells, the phenotype of cells in cluster 0 was less frequent in emphysema and fibrosis than in CF and in emphysema, clusters 4 and 3 were additionally diminished compared to CF (Figure 3a, CD3⁺CD4⁺ panels).

In LN samples (Figure 3b), disease-specific phenotypic configurations among our populations of interest were less pronounced than in LT. Yet,
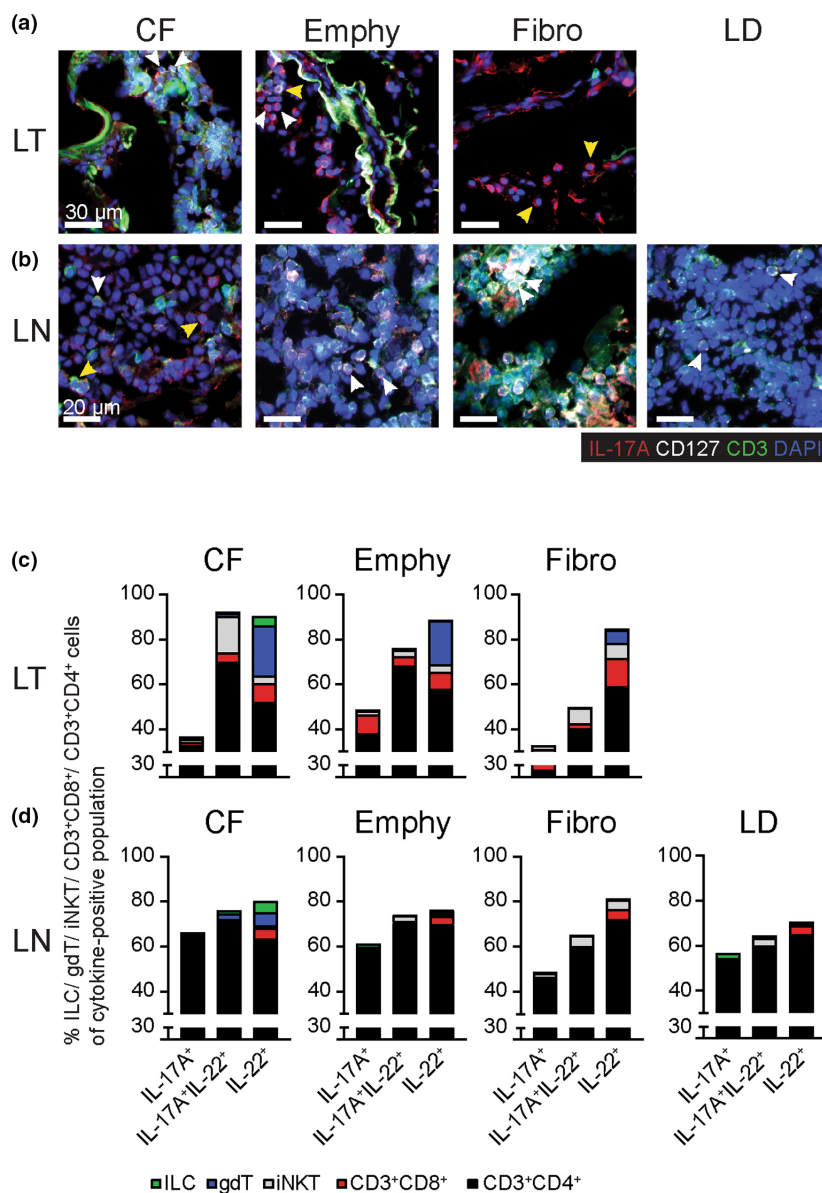
Figure 2. Non-conventional lymphocytes are substantial contributors to IL-17A and IL-22 cytokine production in different end-stage lung diseases. **(a)** Immunofluorescence microscopy of cryo-sections from lung tissue (LT) and **(b)** lymph nodes (LN) of patients with the indicated end-stage lung diseases were stained for IL-17A, CD3, CD127 and with DAPI. White arrowheads: examples of IL-17A$^+$CD3$^+$ cells; yellow arrowheads: examples of IL-17A$^+$CD3$^-$ cells. Please note that arrowheads mark typical examples rather than all cells detected. Images are representative of four or five patients per tissue and disease entity. **(c)** Cellular composition of IL-17A$^+$, IL-17A$^+$IL-22$^+$ and IL-22$^+$ cells in LT and **(d)** LN from CF, fibrosis, emphysema patients and lung donors' LN (LD) as indicated. Please note bottom *y*-axis segments cover values 0–30, upper *y*-axis segments cover values 30–100. CF, cystic fibrosis; Emphy, emphysema; Fibro, idiopathic pulmonary fibrosis; gdT, γδT cells; ILC, innate lymphoid cells; iNKT, iNKT cells.

disease-specific differences were detected in the iNKT cell compartment. Here, cells in cluster 3 originated mostly from CF patients, while cells in cluster 2 originated to a lesser extent from CF samples (Figure 3b, iNKT cell panel). However, among conventional T cells, that is CD4$^+$ and CD8$^+$ T cells, we did not observe any disease-specific

differences and neither for γδ T cells nor ILCs (Figure 3b, see respective panels).

To understand whether disease-specific clusters contained cells with a particularly strong production of IL-17A and/or IL-22, we analysed the average expression of IL-17A and IL-22 in clusters 0–5 separately for every disease and for
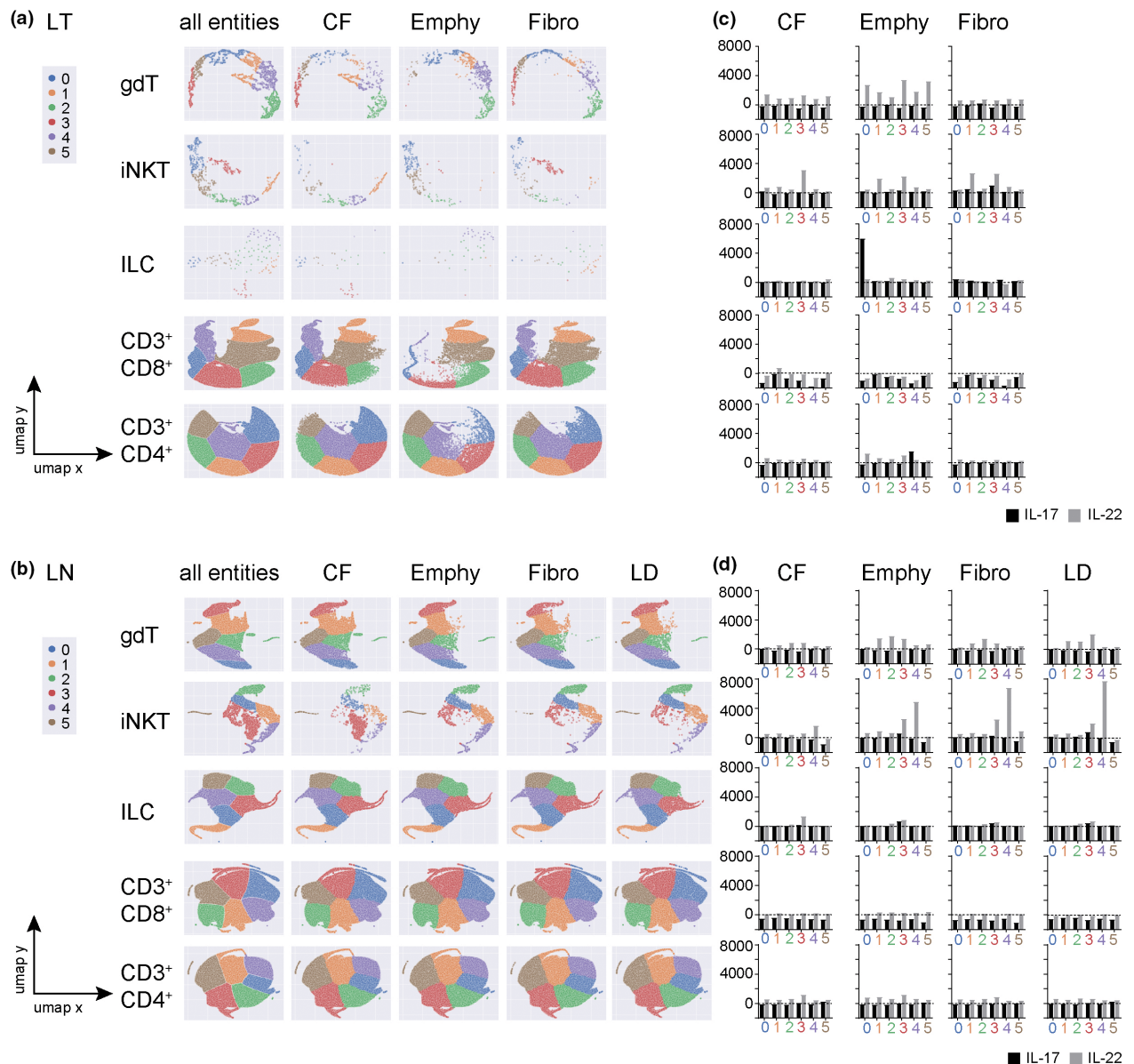
Figure 3. IL-17A-producing non-conventional lymphocyte populations differ between disease entities. **(a)** Lung tissue (LT) and **(b)** lymph node (LN) populations of interest, that is γδ T cells (gdT), iNKT cells, ILC, CD3+CD8+ and CD3+CD4+ cells were identified by manual gating in the flow cytometric data set. Every lymphocyte subpopulation was then subjected to clustering and UMAP (Uniform Manifold Approximation and Projection) depiction based on all markers in the staining panel. In UMAP depictions, one dot represents one cell and identically coloured dots represent cells belonging to the same cluster, with a cluster being defined as a group of cells with similar expression of the markers used for cluster analysis. Please note that because of the design of the analysis, UMAP depictions provide no information on the relative frequency of the different populations of interest (e.g. gdT *vs*. iNKT cells) in the tissues, but only of relative frequencies of cells in clusters 0–5 within the given population of interest (e.g. Cluster 0 cells *vs*. Cluster 1 cells among LT gdT cells). **(c, d)** Average expression of IL-17A and IL-22 in indicated clusters in LT **(c)** and LN **(d)** in individual disease entities. **(a–d)** Data were pooled from 1 to 6 patients per disease, equal numbers of cells per disease, as detailed in the Methods section. CF, cystic fibrosis; Emphy, emphysema; Fibro, idiopathic pulmonary fibrosis; gdT, γδT cells; ILC, innate lymphoid cells; iNKT, iNKT cells; LD, lung donor.

all populations of interest (Figure 3c and d). Indeed, in some cases, we observed that IL-22 production was particularly high in disease-specific clusters; for example, in LT, iNKT cell

cluster 3, consisting of cells, which were most prevalent in fibrosis patients, showed high IL-22 expression across all disease entities (Figure 3c). Similarly, in LN, iNKT cell cluster 3, which

consisted primarily of cells from CF, as well as iNKT cell cluster 4, which contained cells mainly from emphysema, fibrosis and LD patients, showed high expression of IL-22 (Figure 3d). Interestingly, IL-17A expression was similar across most clusters and disease entities, suggesting that IL-17A production is a strongly conserved mediator and redundantly secreted by different phenotypically distinct subclusters within subpopulations of lymphocytes across all three disease entities of end-stage lung disease.

In summary, particularly in γδ T cells and iNKT cells from LT and LN and to a lesser degree in CD3$^+$CD4$^+$ and CD3$^+$CD8$^+$ T cells in LT, we found subclusters more, or exclusively, prevalent in specific end-stage diseases. Some of these subclusters show higher secretion levels of IL-22 than other subclusters, whereas IL-17A secretion was more uniform across all subclusters.

Lymphocytes from CF patients' tissues show the highest IL-17A-associated cytokine signature

To dissect the IL-17A-associated pro-inflammatory environment in different end-stage lung diseases, we measured the secretion of additional IL-17 family cytokines in LT and LN using BioPlex assays and ELISAs and performed unbiased hierarchical clustering of the levels of IL-17A and IL-22 secretion together with the levels of the IL-17A-associated soluble mediators sCD40L, IL-23 and IL-6. Clustering of LT samples based on these cytokine levels resulted in two major clusters comprising patients with either high/medium or with low IL-17A secretion patterns (Figure 4a). The diseases with the highest percentage of patient samples falling into the high/medium producers cluster were CF (57% of samples) and fibrosis (86% of samples), whereas emphysema samples fell predominantly into the 'low' cluster (33% of samples in 'high/medium', 67% of samples in 'low') (Figure 4a). Clustering of LN samples identified three groups with high, intermediate (medium) and low secretion patterns, respectively (Figure 4b). Again, CF samples fell predominantly into the high secretion cluster (70% of samples), confirming the association of CF samples with high levels of IL-17A pathway cytokines, whereas emphysema samples were found equally often in the high (43% of samples) and intermediate producer group (43% of samples), and fibrosis as well as LD

samples located preferentially to the low producer cluster (fibrosis: 60% of samples in 'low', LD: 40% of samples in 'low'). In summary, these analyses found CF to display the most pronounced IL-17A signature of the three end-stage lung disease entities we analysed.

To gain more insight into which signals are driving the cytokine production in the tissues analysed, that is to identify disease-specific contributions of upstream pathways involved in the induction and maintenance of IL-17A,[16] we compared the concentrations of IL-1β, IL-6 and IL-23 in supernatants from LT and LN lymphocytes between the disease entities. In LT, differences in cytokine production between the disease entities showed comparable levels of IL-6, and IL-23, which were higher than secretion of these cytokines by emphysema samples (Figure 4c). IL-β levels were highest in fibrosis samples, which were significantly elevated compared to emphysema samples but not compared to CF samples (Figure 4c).

In end-stage lung-draining LN, the differences were more pronounced and corroborated the high IL-17-family cytokine signature observed in CF samples: IL1β was detected exclusively in CF samples. No statistically significant differences were observed in IL-6 and IL-23 production comparing the disease entities and LD LNs. Nevertheless, both IL-6 and IL-23 concentrations showed very clear trends to be consistently highest in CF LN, lower in emphysema, even lower in fibrosis and lowest in LD LNs (Figure 4d), suggesting that these upstream cytokines underlie the more pronounced IL-17-family cytokine signature we had observed in LN CF samples. Altogether, these results identified CF tissues, particularly the lung-draining LNs, as displaying the most pronounced IL-17-asociated signature, including upstream pathways involved in its induction and maintenance, contributing to previous studies, which describe CF as an 'IL-17 disease'.[23–26]

Microbial colonisation of end-stage lungs is associated with IL-17A and IL-22 production

Conventional culture-dependent microbiological analyses of bronchial secretions obtained intra-operatively revealed higher detection rates of *P.a.*, *S.a.*, fungi and other specific bacterial species in samples from CF patients compared to samples from patients with emphysema or fibrosis (Table 1 and Supplementary figure 1c). Thus, these
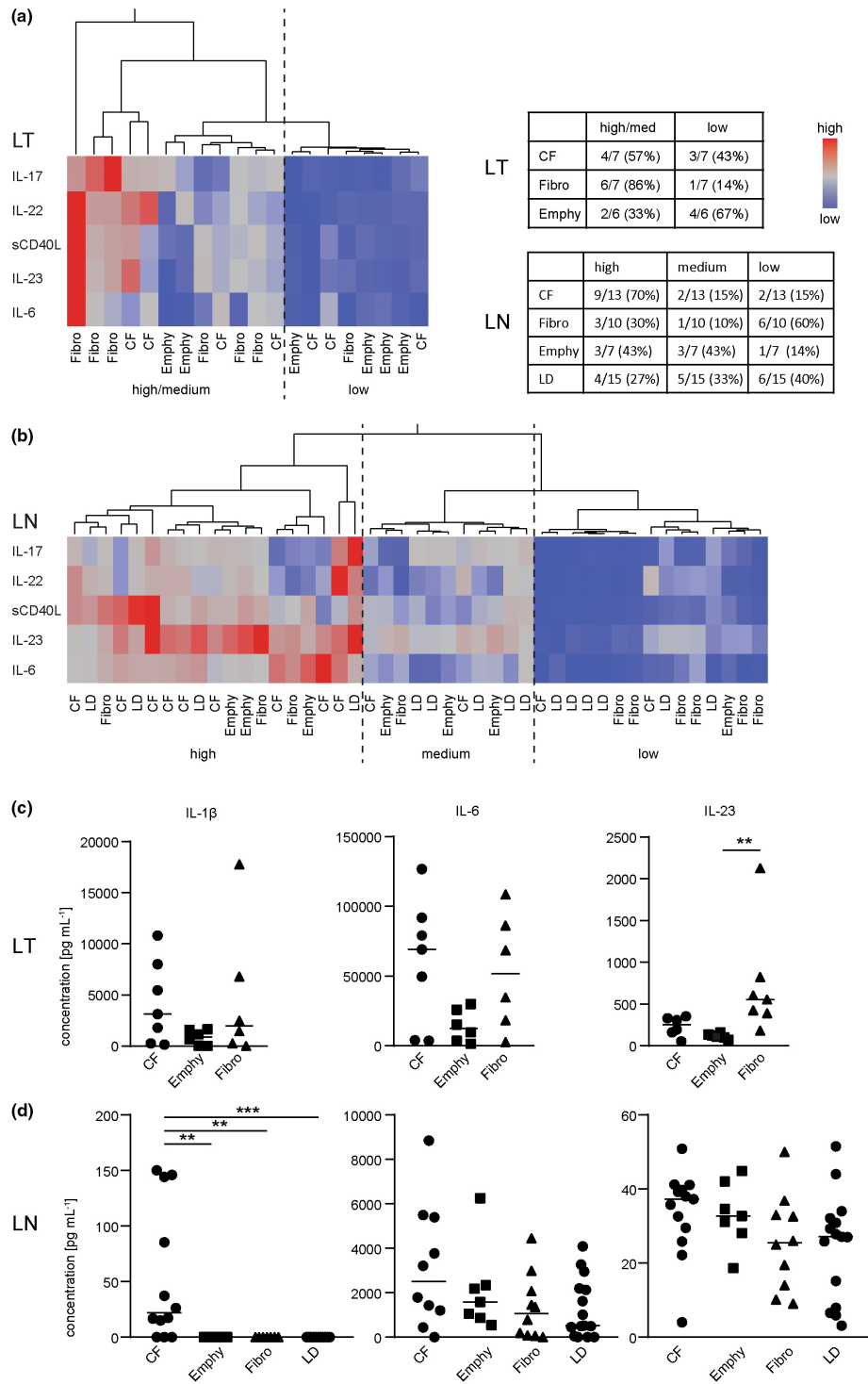
Figure 4. Lymphocytes from CF patients' tissues show the highest IL-17A-associated cytokine signature. **(a, b)** Unbiased hierarchical clustering of concentration levels of IL-17A and IL-22, sCD40L, IL-23 and IL-6 in PMA/ionomycin-re-stimulated supernatants from LT **(a)** and LN **(b)** samples. Tables show numbers and percentages of patient samples allocated to the individual clusters. **(c, d)** Concentrations of IL-1β, IL-6 and IL-23 detected in supernatants from PMA/ionomycin-re-stimulated samples from LT **(c)** and LN **(d)** of patients with CF, emphysema, fibrosis and lung donors' LN (LD). CF, cystic fibrosis; Emphy, emphysema; Fibro, idiopathic pulmonary fibrosis; LD, lung donor; LN, lymph node; LT, lung tissue. **(c, d)** A Kruskal–Wallis test with Dunn's multiple comparisons test was used. Non-indicated pairwise comparisons are n.s.

analyses confirmed CF as the disease entity with the highest level of microbial colonisation, suggesting that microbial colonisation might drive the more pronounced IL-17 family signature observed in CF samples. To substantiate this hypothesis, we measured secretion of IL-17A secretion upon re-stimulation with *P.a.* or *Aspergillus fumigatus* (*A.f.*) extract, focusing on CF *vs.* LD LN samples because of the low levels of microbial colonisation found in emphysema and fibrosis samples, which preclude meaningful comparisons in those entities (Supplementary figure 1c and Table 1). In spite of small overall sample numbers (*P.a.*: $n = 4$ for CF LN and $n = 2$ for LD LN; *A.f.*: $n = 4$ for CF LN and $n = 3$ for LD LN samples), these analyses consistently revealed elevated production of IL-22 and the upstream cytokines IL-1β, IL-6 and IL-23 in antigen-specifically re-stimulated CF samples compared to LD LNs (Figure 5a and b), suggesting that *in situ*, IL-17 family cytokine production is driven by microbial colonisation with *P.a.* or *A.f.* and the ensuing development of antigen-specific T cells.

To also take into account the effect of specific pathogens on the secretion of IL-17A and/or IL-22 by non-T cells, we compared CF samples with the detection of specific pathogens *vs.* samples without the detection of specific pathogens. We focused our analysis on CF samples, in which all pathogens were detectable and of which we had at our disposal a sufficient number of samples with or without detection of the specific pathogens. To test whether microbial colonisation affects the overall levels of IL-17A and IL-22 production, we analysed cytokine concentrations per fixed number of lymphocytes as well as the frequencies of IL-17A-positive or IL-22-positive lymphocytes among total lymphocytes in LT and LN.

In LT, CF patients with the detection of *P.a.* or *S.a.* or *A.f.* consistently displayed higher trends for both IL-17A secretion per 10^6 live lymphocytes and frequencies of IL-17A$^+$ lymphocytes among live lymphocytes (Figure 5c). Results for IL-22 in LT showed similar trends, albeit not regarding *S.a.* detection and IL-22 secretion and fungi and IL-22$^+$ lymphocytes (Figure 5d). Of note, because of the small size of the data set, neither of our measurements, in LT or LN samples, were amenable for statistical testing, so that our conclusions needed to be made based on the trends observed. In bronchial LN, secretion and cytokine-positive lymphocytes were similar and, in most cases, even trended higher in samples from CF patients who

did not have positive *P.a.* or *S.a.* or *A.f.* airway cultures (Figure 5e and f), suggesting that an increased effect of bacterial colonisation may manifest primarily in the LT itself.

DISCUSSION

Our results provide a comprehensive analysis on the secretion patterns of IL-17A- and IL-17A-associated cytokines in three different end-stage lung diseases and dissect the contribution of non-conventional lymphocytes to the secretion of IL-17A and IL-22. We confirm previous data that Th17 cells constitute the most important single contributor to IL-17A and IL-22 secretion in LT and lung-draining LNs.[27] Yet, we demonstrate that significant proportions of non-CD3$^+$CD4$^+$ lymphocytes contribute to IL-17A and/or IL-22 production in LT and LN in all three end-stage lung diseases, we analysed. We furthermore identify disease-specific differences with regard to T- and non-T-lymphocyte contribution to IL-17A, IL-22 and co-secretion in LT and LN. The differences we observed with regard to microbial colonisation and antigen-specific cytokine secretion upon stimulation with *P.a.* and *A.f.* suggest microbial colonisation to drive the more pronounced IL-17 signature in samples from CF patients.

Our analyses of IL-17A and/or IL-22 secretion in supernatants and unbiased hierarchical clustering of secreted IL-17A and associated cytokines indicate a higher propensity for IL-17A and IL-22 secretion in CF samples compared to emphysema and fibrosis samples. Additionally, we identify trends towards higher secretion of IL-1β, IL-23 and IL-6 in CF samples than emphysema and fibrosis samples, suggesting that these cytokines upstream of IL-17A secretion lead to the more pronounced IL-17 signature in CF. Studies on the induction of IL-17A by epithelial signals in response to pathogen-derived danger signals,[1,28] the critical role of IL-17A in defence against airway *P.a.* and *S.a.* infections,[29,30] and its secretion in *A.f.*-associated pathologies,[2] all typical chronic colonisers of CF airways, are corroborated by our data. Our data show higher detection percentages of *P.a.*, *S.a.* and *A.f.* in CF samples (Supplementary figure 1c), reveal higher antigen-specific secretion of IL-17A and associated cytokines in CF samples in response to *P.a.* and *A.f.* compared to LD (Figure 5a and b) and provide evidence for higher secretion levels of IL-17A and IL-22 by lymphocytes from LT samples where *P.a.*, *S.a.* or *A.f.* were detected in intra-operatively obtained bronchial secretions of the
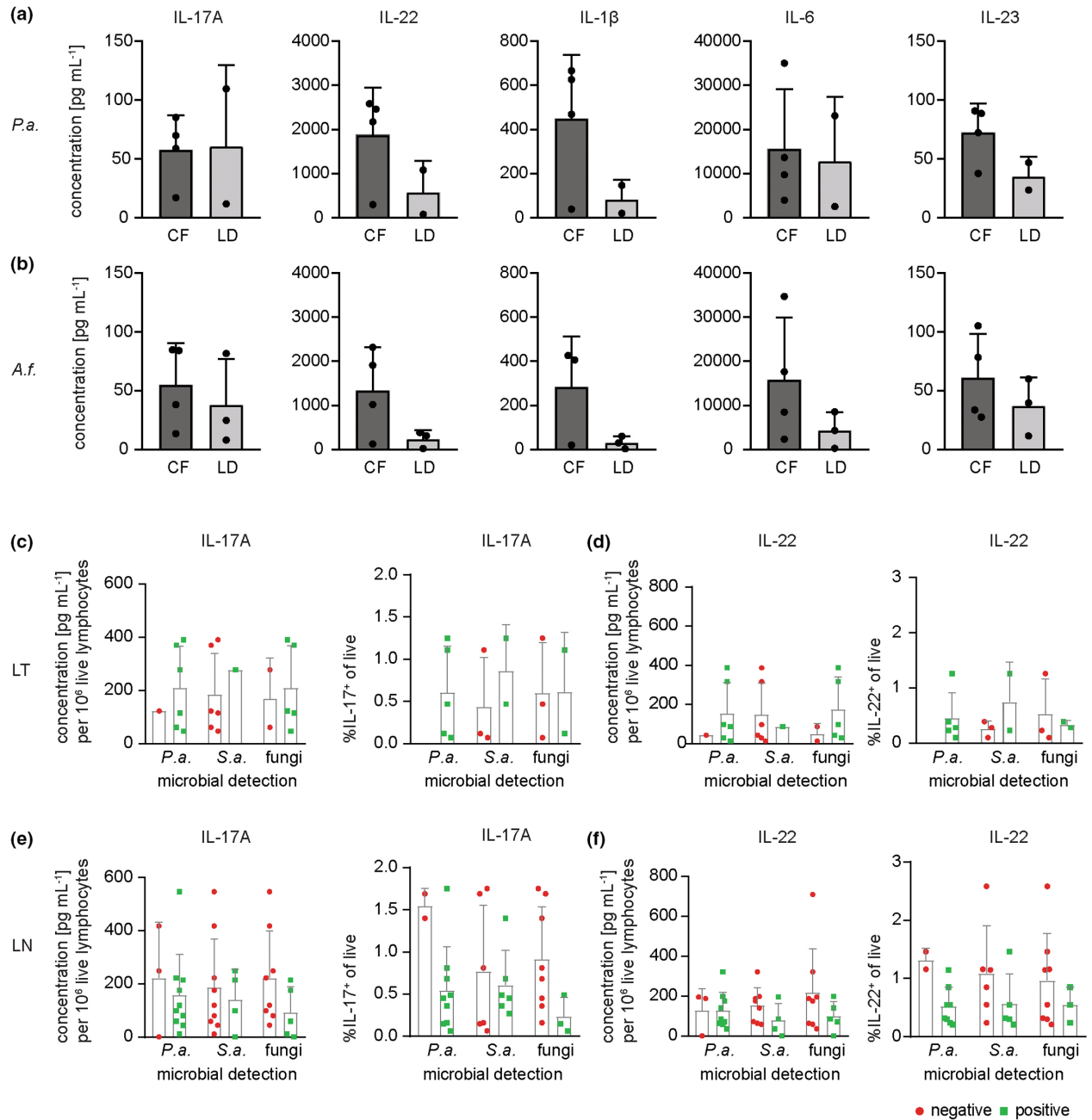
Figure 5. IL-17A secretion is associated with the detection of hallmark airway pathogens in end-stage lung diseases. **(a, b)** Secretion of IL-17A, IL-22, IL-1β, IL-6 and IL-23 in supernatants of lymphocytes isolated from cystic fibrosis (CF) LN and lung donor (LD) LN upon re-stimulation with *Pseudomonas aeruginosa* (*P.a.*) extract **(a)** or *Aspergillus fumigatus* (*A.f.*) extract **(b)**. Every dot indicates one patient sample. A Mann–Whitney test was used for all comparisons in **a** and **b**, where feasible, n.s. **(c)** IL-17A concentrations and %IL-17A+ cells among LT lymphocytes and **(d)** IL-22 concentrations and %IL-22+ cells among LT lymphocytes from CF patients with (green bars + symbols) or without (red bars + symbols) detection of *P.a.*, *Staphylococcus aureus* (*S.a.*) or *Aspergillus* species. **(e)** IL-17A concentrations and %IL-17A+ cells among LN lymphocytes and **(d)** IL-22 concentrations and %IL-22+ cells among LN lymphocytes from CF patients with (green bars + symbols) or without (red bars + symbols) detection of *P.a.*, *S.a.* or *Aspergillus* species. Statistical testing was not applicable because of small size of data set **(c–f)**. LN, lymph node; LT, lung tissue.

patients (Figure 5c and d). Our results thus confirm findings on a highly pro-inflammatory milieu in CF samples[24,31–33] and on increased IL-17A and IL-22 levels and co-secretion in CF sputum, LN samples,[23,34,35] BAL and bronchial biopsies.[26] Taken together, they suggest that the over-abundance of

IL-17A in CF samples likely reflects the hierarchy of pro-inflammatory, microbial 'pressure' for the three disease entities studied.

Apart from the described differences between the three disease entities, our results also identify similarities across the three disease entities. For example, the relative contribution of non-conventional lymphocyte populations compared to conventional T lymphocytes to IL-17A and IL-22 secretion is consistently less in LN in comparison with LT (Figure 2d cf. c). Also, regardless of disease entity and tissue origin, the relative contribution of non-T-lymphocytes compared to conventional T lymphocytes was consistently higher with regard to IL-22 production or IL-17A/IL-22 co-production than IL-17A production alone (Figure 2c and d). Our results thus reveal that IL-17A and IL-22 contribute to the pro-inflammatory microenvironment of all three end-stage lung disease entities and might constitute a converging inflammatory pathway of the end-stage lung processes involved in CF, emphysema and fibrosis.

Our finding that γδ T cells and iNKT cells are sources of IL-22 in all three diseases indicates that induction of IL-22 secretion in end-stage lung disease is achieved by damage- or pathogen-associated molecular pattern recognition in γδ T cells and *via* lipid binding of CD1d in iNKT cells.[36,37] Thus, in end-stage lung disease synergistic homeostatic IL-22 secretion occurs in the context of infection (pathogen-associated) and breach of tissue integrity (lipids), pointing to overlapping mechanisms towards tissue repair by processes commonly found in end-stage lung diseases. Yet, the pro-regenerative properties of IL-22 are ultimately insufficient in the end-stage disease states we studied, where tissue destruction is a common endpoint of CF, emphysema and idiopathic fibrosis lung disease. In that line, Si-Tahar and colleagues demonstrated that neutrophil- and macrophage-derived proteases can inactivate IL-22 in CF samples,[38] suggesting an imbalance of pro-inflammatory IL-17A *vs.* reparative IL-22 in CF lung disease. IL-17A has been implicated in neutrophilic inflammation,[22] mucus production,[39] and lung damage,[22,28,40] indicating mechanisms by which IL-17A exerts a critical influence on the progression towards end-stage lung disease in CF. As we showed that IL-17A and IL-22 are present in all three end-stage lung diseases, IL-22's ability to counteract fibrosis[36] might be short-circuited by IL-17A in all three lung diseases. By mechanisms similar to

those observed in CF lung disease,[22,38] IL-17A might thus play a critical role in the progression of fibrosis in all end-stage lung diseases.

Finally, IL-17A and IL-22 critically affect the development of tertiary lymphoid follicles in LT.[7–9,41,42] Both cytokines have also been implicated in B-cell migration[43] in the context of germinal centre formation and B-cell recruitment.[6] These findings point towards another possible common mechanism by which IL-17A and IL-22 could contribute to end-stage lung disease progression. Our data on secretion of IL-17A and/or IL-22 in LN samples from all three end-stage lung disease samples analysed suggest that IL-17A and IL-22 might influence not only BALT formation in LT but also the overall humoral immune response *via* their effects in LNs in end-stage lung disease. The association between autoimmune antibodies and progression of chronic obstructive pulmonary disease (COPD),[44] CF[45] and idiopathic pulmonary fibrosis[46] suggests the breakdown of immunological tolerance and ensuing autoantibody production as a common feature in the progression towards end-stage disease. It will be of interest to investigate further the specific role of ILCs in this context, which we found in significant frequencies among the IL-17A- and/or IL-22-secreting lymphocytes in LN samples from CF and emphysema patients. Our data suggest a unique role for these cells in humoral immune responses in LNs in the context of chronic respiratory infections beyond their known role in neutrophil-mediated lung injury in LT.[32]

Taken together, we provide a comprehensive analysis of IL-17A-associated responses in end-stage lung diseases by directly comparing material originating from emphysema and idiopathic fibrosis or CF patients. One inherent shortcoming of our analyses is the overall low sample numbers, inherent age discrepancies between the different disease entities (Supplementary figure 1a) and overall high inter-patient variability. We were able to address inter-patient variability by quality criteria (e.g. outlier testing) employed to exclude samples before comprehensive analysis and normalisation approaches, although these stringent quality control measures furthermore reduced sample size. Given our unique lung transplantation programme, which allowed us to acquire and analyse a yet unreported number of samples, the combination with these diligent quality controls and the normalisation strategies, we believe that we present

a state-of-the-art data set and analysis, which, keeping in mind the abovementioned deficiencies, can substantially contribute to its field.

In summary, our data suggest that different lymphocyte subpopulations secrete IL-17A and IL-22 – triggered by infectious and non-infectious mechanisms, which converge in end-stage lung diseases and thus provide an IL-17A-enriched milieu promoting progression of tissue destruction and fibrosis. Because of increased microbial load, these mechanisms appear to be most pronounced in CF patients where the development of end-stage disease might thereby be accelerated.

METHODS

Patient material and characteristics

Bronchial lymph node (LN) and lung tissue (LT) samples were obtained from explanted native lungs of patients with CF, emphysema or idiopathic pulmonary fibrosis, respectively, at the time of lung transplantation. Patient characteristics are detailed in Table 1, Supplementary figure 1a–c and in the first paragraph of the Results section (Patient characteristics). LT samples were sized to a standard of 3–5 cm^3 and chosen to contain intersegmental bronchi or bronchioli. Preparation of single-cell suspensions from these samples is described below. Sample acquisition was approved by the local ethics committee (Ethical approval #2700-2015). Twenty-one of the 23 CF samples were subjected to additional analyses published elsewhere.[22] LN from lung donors (LD) was obtained from the donor trachea during lung transplantation as described in the first paragraph of the Results section.

Bronchial secretions were obtained intra-operatively during transplantation and cultured according to standard microbiological practice for the detection of bacteria and fungi. These analyses detected specific pathogens: fungi (*Aspergillus* species, *Saccharomyces* species, *Candida* species and *Wangiella* species) and bacteria: (*Pseudomonas aeruginosa*, *Staphylococcus aureus*) and 'other' specific bacterial species (*Achromobacter*, *Burkholderia*, *Stenotrophomonas*, *Enterococcus*, *Serratia*, *Escherichia*, *Enterobacter*, *Haemophilus* and *Klebsiella*).

Preparation of human tissue samples for flow cytometry

LT and LN specimens were stored in cell culture medium with FCS (lymph nodes) and antibiotics and antimycotics (lung tissue; 2.5 µg mL^{-1} Amphotericin B, Bristol-Myers Squibb, New York City, NY, USA; 1 µg mL^{-1} Voriconazol Eberth, Ursensollen, Germany) at 4°C before processing. LT specimens were disrupted with gentleMACS dissociator (Miltenyi, Bergisch Gladbach, Germany) and incubated for 35 min in 37°C in digestion buffer (RPMI, 2.5% FCS, 2 mg mL^{-1} Collagenase (Type III, Worthington; Worthington Biochemical Corporation, Lakewood, NJ, USA)) and 10 µg mL^{-1} DNase I (Sigma-Aldrich, Taufkirchen,

Germany). Digestion was stopped by adding EDTA to a final concentration of 0.01 mM. LN specimens were mechanically cut into pieces. Single-cell suspensions were generated by grinding LT digests and LN pieces through a metal mesh and cell strainer (100 µm, Greiner Bio-One, Kremsmünster, Austria) followed by red blood cell lysis. Samples were consecutively split evenly and re-stimulated for either (1) flow cytometric analyses of intracellular cytokine secretion or (2) measurements of cytokines in cell cultures supernatants.

Flow cytometry

For flow cytometric staining of IL-17 and IL-22, LT and LN single-cell suspensions were adjusted to 1×10^7 cells mL^{-1} and incubated for 4 h with PMA (0.1 µg mL^{-1}; Sigma-Aldrich) and ionomycin (0.75 µg mL^{-1}; Sigma-Aldrich) in the presence of Golgi-Plug (BD). After blocking (human TruStain FcX; BioLegend) and viable stain (Pacific Orange; Thermo Fisher), True Nuclear Buffer kit (BioLegend) was used for washing and cell permeabilisation throughout flow cytometry staining (for antibodies, staining panels and analysis strategy, see Supplementary figure 2). Data were acquired using a FACS Canto (BD) and analysed using FlowJo software (version 10; Treestar).

Cytokine measurements with multiplex and ELISA

For non-specific re-stimulation, LT and LN single-cell suspensions were incubated with PMA and ionomycin as described in the Flow cytometry section above, but in the absence of Golgi-Plug. For antigen-specific re-stimulation, LN single-cell suspensions were adjusted to 10^7 cells mL^{-1} in IMDM supplemented with 10% FCS, L-glutamine, Penicillin/Streptomycin, β-mercaptoethanol, Voriconazol (1 µg mL^{-1}) and Amphotericin B (2.5 µg mL^{-1}), and IL-2 (1.7×10^4 U mL^{-1}). *P.a.* extract (prepared by sonication and heat-inactivation of *P.a.* strain PAO1, courtesy of Nina Cramer, Hannover Medical School, Germany) or *A.f.* extract (Greer Laboratories, Lenoir, NC, USA) was added at final concentration of 1 or 5 µg mL^{-1}, respectively, and cells were incubated for 6–7 days, with medium addition on day 1 and day 4. Supernatants were collected thereafter. Cytokines were quantified using Bio-Plex Pro™ Human Th17 Cytokine Panel 15-Plex (Bio-Rad). IL-1β, IL-6 and TNFα concentrations exceeded upper limit of detection in multiplex assays and were measured in diluted supernatants using ELISA kits (ELISA MAX; BioLegend). All cytokine concentration values determined in re-stimulated supernatants were normalised to 10^6 live lymphocytes based on the cell number seeded per well and the percentage of live lymphocytes assessed by flow cytometric analysis of the same sample. For those samples for which flow cytometric information was not available, normalisation of the cytokine concentrations was performed based on the average percentage of live lymphocytes among across all samples in that particular disease entity. All analyses were subjected to quality control measures excluding samples with an unusually low cell viability as well as outlier values based on the ROUT test (GraphPad Prism) as described below in Statistics.

Immunofluorescence microscopy

LN and LT samples were frozen in O.C.T. compound (Tissue-Tek; Sakura Finetek, Umkirch, Germany) and stored at −80°C. Tissue sections of 6–8 μm thickness were prepared on a Cryo-microtome (Leica) and transferred onto HistoBond adhesive glass microscope slides (Marienfeld, Lauda-Königshofen, Germany). Sections were dried for at least 1 h at RT and fixed for 10 min using 4% paraformaldehyde in PBS (pH = 7.4) at 4°C. Sections were stained on the same day. For immunofluorescence staining, sections were re-hydrated using PBS with 0.1% Tween (PBS-T) and blocked with 5% donkey serum, followed by incubation with mouse anti-human–IL-17A antibody (R&D MAB3171, Monoclonal Mouse IgG$_1$ Clone #41802), washing with PBS-T; incubation with secondary donkey anti-mouse AlexaFluor647 antibody (Invitrogen A3171), washing with PBS-T and blocking with 2.5% mouse serum; incubation with anti-CD3 (mouse anti-human CD3; BioLegend 300440) and anti-CD127 (mouse anti-human CD127; Beckman, IM1980U) antibodies, washing with PBS-T; incubation with DAPI (1 μg mL^{-1}); and a final washing step with PBS-T. Samples were mounted for acquisition using Immu-Mount (Fisher Scientific). All incubations were performed at RT. For control purposes, unstained and secondary antibody only controls were generated in parallel. Images were acquired on a ZEISS Observer microscope.

Hierarchical clustering and unsupervised cluster analyses

Euclidean distance analysis and ward algorithm were applied to generate unbiased hierarchical clusters in JMP software (version 12; SAS Institute Inc.).

For unsupervised cluster analysis, cells from LN and LT of patients with CF, emphysema or fibrosis were analysed by FACS staining. The populations of interest (CD4$^+$ T cells, CD8a$^+$ T cells, γδ T cells, ILCs and iNKT cells, for gating strategy refer to Supplementary figure 2) were identified by manual gating and expression values of all markers of the flow cytometry staining panel of the chosen cell populations were exported for cluster analysis using FlowJo (Scale values). Markers included in the clustering thus were as follows:

1. IL-17A, IL-22, CD3, CD4, CD8, CCR7 and CD45RA for CD4$^+$ T cells and CD8$^+$ T cells;
2. IL-17, IL-22, CD3, Lineage Mix (CD11c CD14 CD19), RORg, gdTCR and iNKT-TCR for gdT cells and iNKT cells; and
3. IL-17, IL-22, CD3, Lineage Mix (CD11c CD4 CD14 CD19), RORg, CD127 and NKp46 for ILCs.

We prepared UMAP depictions, in which every cluster represents a specific cellular state ('phenotype') within the analysed population. For example, in cluster analyses of ILCs, those ILCs with a similar expression of the markers used for clustering locate to the same cluster, denoted by a separate colour of the dots. The number of cells (dots) in one cluster represents the number of cells in that particular 'state'. Hence, 'large' clusters, that is clusters containing many cells (dots), represent cellular states or phenotypes that are typical of the cell type and disease analysed. These analyses thus permit comparisons of the relative frequencies of specific clusters between different disease entities. Of note, however, these analyses do not provide information on relative frequencies of ILCs, γδ T cells, iNKT, CD3$^+$CD8$^+$ or CD3$^+$CD4$^+$ cells among IL-17A or IL-22 producing lymphocytes since CD4$^+$ T cells, CD8$^+$ T cells, γδ T cells, iNKT cells and ILCs were separated from another by manual gating of the flow cytometry data prior to clustering.

To prevent any bias in the selection of cells for cluster analysis, we performed downsampling calculations to select the same number of cells from every disease. Based on the cell counts, we defined a threshold for the complete exclusion of samples (e.g. < 100 cells), for the complete inclusion of samples (e.g. 100–500 cells), and for the downsampling of samples (e.g. > 500 cells). We then sought to include the same amount of cells from all patients as well as to include cells from at least three patients per disease entity where possible. These calculations were performed separately for every combination of disease/population of interest/organ, so that a maximum number of total cells could be included in the analyses. Thus, we succeeded in including three or more patients for all analyses except LT samples from emphysema. The final number of patient samples included in the analysis were as follows: for LT: *n*(CF) = 3 or 4, *n*(emphy) = 1 or 2, *n*(fibro) = 3; for LN: *n*(CF) = 4, *n*(emphy) = 5 or 6, *n*(fibro) = 8, *n*(LD) = 6.

On the selected data, a dimensionality reduction using UMAP (umap-learn, 0.3.10, using default arguments) was done. Then, to identify disease-specific clusters the reduced data were clustered using Gaussian Mixture Models (GMM, Python 3.7.3, scikit-learn 0.21.1), with 6 as the number of components. To determine the optimal number of components for the data, the Bayesian information criterion (BIC) was calculated for possible number of components between 2 and 15. Using this method, six clusters were found to be optimal.

The resulting clusters were visualised in a UMAP-Plot displaying all cells from all three disease entities (all entities). Next, to identify which disease entities contributed to which clusters, UMAP-Plots were generated displaying cells from the individual diseases only.

Statistics

Statistical significance was calculated using GraphPad Prism version 9.0.0 for Windows, GraphPad software. Outliers within groups were eliminated using the ROUT test (GraphPad software). The statistical tests, which were applied, are given in the figure legends. For the analyses shown in Supplementary figure 1c, individual panels in Figure 5a and b and in Figure 5c–f, statistical testing was not feasible because of the limited sized of the data set, which did not fulfil the criteria of the applicable tests. For statistical tests, a *P*-value limit of *P* < 0.05 was accepted to indicate statistical significance. In figures, asterisks indicate *P* < 0.05 (*), *P* < 0.01 (**) and *P* < 0.001 (***), and *P* > 0.05 (n.s., not significant), respectively.

ACKNOWLEDGMENTS

CONFLICT OF INTEREST

The authors declare no conflict of interest.

AUTHOR CONTRIBUTIONS

Melanie Albrecht: Conceptualization; data curation; formal analysis; funding acquisition; investigation; methodology; project administration; supervision; validation; visualization; writing – original draft; writing – review and editing. **Olga Halle:** Conceptualization; data curation; formal analysis; investigation; methodology; project administration; supervision; validation; visualization; writing – original draft; writing – review and editing. **Svenja Gaedcke:** Data curation; formal analysis; investigation; methodology; visualization; writing – review and editing. **Sophia T Pallenberg:** Data curation; formal analysis; investigation; writing – review and editing. **Julia Camargo Neumann:** Investigation. **Marius Witt:** Investigation. **Johanna Roediger:** Investigation. **Marina Schumacher:** Formal analysis; investigation. **Adan Chari Jirmo:** Conceptualization; formal analysis; investigation; methodology; visualization; writing – review and editing. **Gregor Warnecke:** Methodology; resources. **Danny Jonigk:** Funding acquisition; methodology; resources; writing – review and editing. **Peter Braubach:** Data curation; investigation; methodology; resources. **David DeLuca:** Formal analysis; methodology; supervision. **Gesine Hansen:** Conceptualization; funding acquisition; resources. **Anna-Maria Dittrich:** Conceptualization; formal analysis; funding acquisition; investigation; methodology; project administration; resources; supervision; writing – original draft; writing – review and editing.

REFERENCES

1. McAleer JP, Kolls JK. Directing traffic: IL-17 and IL-22 coordinate pulmonary immune defense. *Immunol Rev* 2014; **260**: 129–144.
2. Bacher P, Hohnstein T, Beerbaum E *et al*. Human anti-fungal Th17 immunity and pathology rely on cross-reactivity against *Candida albicans*. *Cell* 2019; **176**: 1340–1355 e1315.
3. Alcorn JF. IL-22 plays a critical role in maintaining epithelial integrity during pulmonary infection. *Front Immunol* 2020; **11**: 1160.
4. Fleige H, Ravens S, Moschovakis GL *et al*. IL-17-induced CXCL12 recruits B cells and induces follicle formation in BALT in the absence of differentiated FDCs. *J Exp Med* 2014; **211**: 643–651.
5. Barone F, Nayar S, Campos J *et al*. IL-22 regulates lymphoid chemokine production and assembly of tertiary lymphoid organs. *Proc Natl Acad Sci USA* 2015; **112**: 11024–11029.
6. Tanaka S, Gauthier JM, Fuchs A *et al*. IL-22 is required for the induction of bronchus-associated lymphoid tissue in tolerant lung allografts. *Am J Transplant* 2020; **20**: 1251–1261.
7. MacDonald KP, Blazar BR, Hill GR. Cytokine mediators of chronic graft-versus-host disease. *J Clin Invest* 2017; **127**: 2452–2463.
8. Grogan JL, Ouyang W. A role for Th17 cells in the regulation of tertiary lymphoid follicles. *Eur J Immuno* 2012; **42**: 2255–2262.
9. Celada LJ, Kropski JA, Herazo-Maya JD *et al*. PD-1 up-regulation on CD4^{+} T cells promotes pulmonary fibrosis through STAT3-mediated IL-17A and TGF-β1 production. *Sci Transl Med* 2018; **10**: eaar8356.
10. Varelias A, Gartlan KH, Kreijveld E *et al*. Lung parenchyma-derived IL-6 promotes IL-17A-dependent acute lung injury after allogeneic stem cell transplantation. *Blood* 2015; **125**: 2435–2444.
11. Li Q, Gu Y, Tu Q, Wang K, Gu X, Ren T. Blockade of Interleukin-17 restrains the development of acute lung injury. *Scand J Immunol* 2016; **83**: 203–211.
12. Francois A, Gombault A, Villeret B *et al*. B cell activating factor is central to bleomycin- and IL-17-mediated experimental pulmonary fibrosis. *J Autoimmunity* 2015; **56**: 1–11.
13. Chen Y, Li C, Weng D *et al*. Neutralization of interleukin-17A delays progression of silica-induced lung inflammation and fibrosis in C57BL/6 mice. *Toxicol Appl Pharmacol* 2014; **275**: 62–72.
14. Lammertyn EJ, Vandermeulen E, Bellon H *et al*. End-stage cystic fibrosis lung disease is characterised by a diverse inflammatory pattern: an immunohistochemical analysis. *Respir Res* 2017; **18**: 10.
15. Harrington LE, Hatton RD, Mangan PR *et al*. Interleukin 17-producing CD4^{+} effector T cells develop via a lineage distinct from the T helper type 1 and 2 lineages. *Nat Immunol* 2005; **6**: 1123–1132.
16. Cua DJ, Tato CM. Innate IL-17-producing cells: the sentinels of the immune system. *Nat Rev Immunol* 2010; **10**: 479–489.
17. Fan X, Rudensky AY. Hallmarks of tissue-resident lymphocytes. *Cell* 2016; **164**: 1198–1211.
18. Liu J, Qu H, Li Q, Ye L, Ma G, Wan H. The responses of gammadelta T-cells against acute *Pseudomonas aeruginosa* pulmonary infection in mice via interleukin-17. *Pathog Dis* 2013; **68**: 44–51.
19. Muir R, Osbourn M, Dubois AV *et al*. Innate lymphoid cells are the predominant source of IL-17A during the early pathogenesis of acute respiratory distress syndrome. *Am J Respir Crit Care Med* 2016; **193**: 407–416.
20. Van Maele L, Carnoy C, Cayet D *et al*. Activation of type 3 innate lymphoid cells and interleukin 22 secretion in the lungs during *Streptococcus pneumoniae* infection. *J Infect Dis* 2014; **210**: 493–503.
21. Murdoch JR, Lloyd CM. Resolution of allergic airway inflammation and airway hyperreactivity is mediated by IL-17-producing γδT cells. *Am J Respir Crit Care Med* 2010; **182**: 464–476.
22. Hagner M, Albrecht M, Guerra M *et al*. IL-17A from innate and adaptive lymphocytes contributes to inflammation and damage in cystic fibrosis lung disease. *Eur Respir J* 2021; **57**: 1900716.

23. Chan YR, Chen K, Duncan SR *et al.* Patients with cystic fibrosis have inducible IL-17⁺IL-22⁺ memory cells in lung draining lymph nodes. *J Allergy Clinic Immunol* 2013; **131**: 1117–1129, 1129 e1111–1115.

24. Decraene A, Willems-Widyastuti A, Kasran A, De Boeck K, Bullens DM, Dupont LJ. Elevated expression of both mRNA and protein levels of IL-17A in sputum of stable cystic fibrosis patients. *Respir Res* 2010; **11**: 177.

25. Mulcahy EM, Hudson JB, Beggs SA, Reid DW, Roddam LF, Cooley MA. High peripheral blood th17 percent associated with poor lung function in cystic fibrosis. *PLoS One* 2015; **10**: e0120912.

26. Tan HL, Regamey N, Brown S, Bush A, Lloyd CM, Davies JC. The Th17 pathway in cystic fibrosis lung disease. *Am J Respir Crit Care Med* 2011; **184**: 252–258.

27. Vanaudenaerde BM, Verleden SE, Vos R *et al.* Innate and adaptive interleukin-17-producing lymphocytes in chronic inflammatory lung disorders. *Am J Respir Crit Care Med* 2011; **183**: 977–986.

28. Lore NI, Bragonzi A, Cigana C. The IL-17A/IL-17RA axis in pulmonary defence and immunopathology. *Cytokine Growth Factor Rev* 2016; **30**: 19–27.

29. Tiringer K, Treis A, Fucik P *et al.* A Th17- and Th2-skewed cytokine profile in cystic fibrosis lungs represents a potential risk factor for *Pseudomonas aeruginosa* infection. *Am J Respir Crit Care Med* 2013; **187**: 621–629.

30. Dubin PJ, Martz A, Eisenstatt JR, Fox MD, Logar A, Kolls JK. Interleukin-23-mediated inflammation in *Pseudomonas aeruginosa* pulmonary infection. *Infect Immun* 2012; **80**: 398–409.

31. Osika E, Cavaillon JM, Chadelat K *et al.* Distinct sputum cytokine profiles in cystic fibrosis and other chronic inflammatory airway disease. *Eur Respir J* 1999; **14**: 339–346.

32. Falco A, Romano M, Iapichino L, Collura M, Davi G. Increased soluble CD40 ligand levels in cystic fibrosis. *J Thromb Haemost* 2004; **2**: 557–560.

33. Nixon LS, Yung B, Bell SC, Elborn JS, Shale DJ. Circulating immunoreactive interleukin-6 in cystic fibrosis. *Am J Respir Crit Care Med* 1998; **157**: 1764–1769.

34. McAllister F, Henry A, Kreindler JL *et al.* Role of IL-17A, IL-17F, and the IL-17 receptor in regulating growth-related oncogene-α and granulocyte colony-stimulating factor in bronchial epithelium: implications for airway inflammation in cystic fibrosis. *J Immunol* 2005; **175**: 404–412.

35. Aujla SJ, Chan YR, Zheng M *et al.* IL-22 mediates mucosal host defense against Gram-negative bacterial pneumonia. *Nat Med* 2008; **14**: 275–281.

36. Bendelac A, Lantz O, Quimby ME, Yewdell JW, Bennink JR, Brutkiewicz RR. CD1 recognition by mouse NK1⁺ T lymphocytes. *Science* 1995; **268**: 863–865.

37. Zheng J, Liu Y, Lau YL, Tu W. γδ-T cells: an unpolished sword in human anti-infection immunity. *Cell Mol Immunol* 2013; **10**: 50–57.

38. Guillon A, Brea D, Luczka E *et al.* Inactivation of the interleukin-22 pathway in the airways of cystic fibrosis patients. *Cytokine* 2019; **113**: 470–474.

39. Newcomb DC, Boswell MG, Sherrill TP *et al.* IL-17A induces signal transducers and activators of transcription-6-independent airway mucous cell metaplasia. *Am J Respir Cell Mol Biol* 2013; **48**: 711–716.

40. Roos AB, Sethi S, Nikota J *et al.* IL-17A and the promotion of neutrophilia in acute exacerbation of chronic obstructive pulmonary disease. *Am J Respir Crit Care Med* 2015; **192**: 428–437.

41. Ferretti E, Ponzoni M, Doglioni C, Pistoia V. IL-17 superfamily cytokines modulate normal germinal center B cell migration. *J Leukoc Biol* 2016; **100**: 913–918.

42. Yadava K, Pattaroni C, Sichelstiel AK *et al.* Microbiota promotes chronic pulmonary inflammation by enhancing IL-17A and autoantibodies. *Am J Respir Crit Care Med* 2016; **193**: 975–987.

43. Mountz JD, Wang JH, Xie S, Hsu HC. Cytokine regulation of B-cell migratory behavior favors formation of germinal centers in autoimmune disease. *Discov Med* 2011; **11**: 76–85.

44. Caramori G, Ruggeri P, Di Stefano A *et al.* Autoimmunity and COPD: clinical implications. *Chest* 2018; **153**: 1424–1431.

45. Yadav R, Linnemann RW, Kahlenberg JM, Bridges LS Jr, Stecenko AA, Rada B. IgA autoantibodies directed against self DNA are elevated in cystic fibrosis and associated with more severe lung dysfunction. *Autoimmunity* 2020; **53**: 476–484.

46. Hoyne GF, Elliott H, Mutsaers SE, Prele CM. Idiopathic pulmonary fibrosis and a role for autoimmunity. *Immunol Cell Biol* 2017; **95**: 577–583.
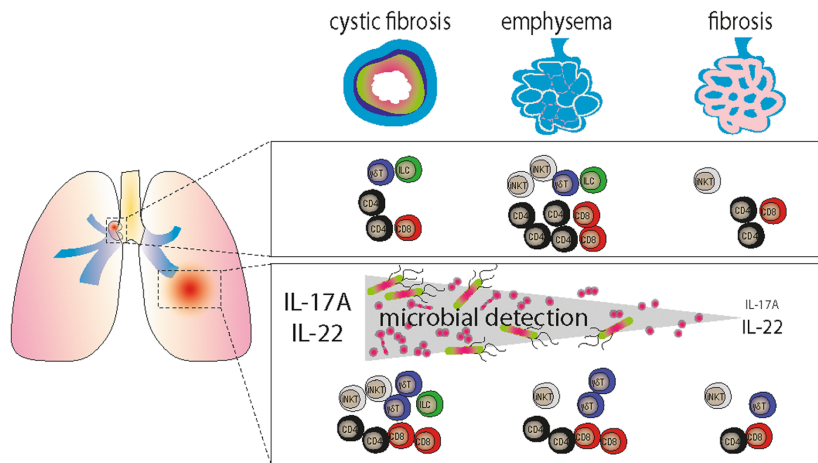
Supporting Information

Additional supporting information may be found online in the Supporting Information section at the end of the article.

Graphical Abstract

The contents of this page will be used as part of the graphical abstract
of html only. It will not be published as part of main.

Our results show that both adaptive and innate lymphocyte populations contribute to IL-17A-dependent pathologies in different end-stage lung disease entities, where they establish an IL-17A-rich microenvironment. Microbial colonisation patterns and cytokine secretion upon microbial re-stimulation suggest that pathogens drive IL-17A secretion patterns in end-stage lung disease.